

1  
2  
3 **Analytical characterization and pharmacological evaluation of the new**  
4 **psychoactive substance 4-fluoromethylphenidate (4F-MPH) and**  
5 **differentiation between the (±)-*threo*- and (±)-*erythro*- diastereomers.**  
6  
7

8 Gavin McLaughlin,<sup>a,b\*</sup> Noreen Morris,<sup>a</sup> Pierce V. Kavanagh,<sup>b</sup> John D. Power,  
9 <sup>b,c</sup> Geraldine Dowling,<sup>b,d</sup> Brendan Twamley,<sup>e</sup> John O'Brien,<sup>e</sup> Gary Hessman,  
10 <sup>e</sup> Brian Murphy,<sup>d</sup> Donna Walther,<sup>f</sup> John S. Partilla,<sup>f</sup> Michael H. Baumann,<sup>f</sup>  
11 and Simon D. Brandt<sup>g</sup>  
12  
13

14  
15  
16 <sup>a</sup> *Department of Life and Physical Sciences, School of Science, Athlone Institute of*  
17 *Technology, Dublin Road, Westmeath, Ireland*

18  
19 <sup>b</sup> *Department of Pharmacology and Therapeutics, School of Medicine, Trinity Centre for*  
20 *Health Sciences, St. James's Hospital, Dublin 8, Ireland*

21  
22 <sup>c</sup> *Forensic Science Ireland, Garda HQ, Phoenix Park, Dublin 8, Ireland*

23  
24 <sup>d</sup> *School of Chemical and Pharmaceutical Sciences, Dublin Institute of Technology, Dublin 2,*  
25 *Ireland*

26  
27 <sup>e</sup> *School of Chemistry, Trinity College Dublin, Dublin 2, Ireland*

28  
29 <sup>f</sup> *Designer Drug Research Unit of the Intramural Research Program, National Institute on*  
30 *Drug Abuse, National Institutes of Health, Baltimore, MD 21224, USA*

31  
32 <sup>g</sup> *School of Pharmacy and Biomolecular Sciences, Liverpool John Moores University, Byrom*  
33 *Street, Liverpool L3 3AF, UK*  
34  
35

36  
37  
38 \*Correspondence to: Gavin McLaughlin, Department of Pharmacology &  
39 Therapeutics, School of Medicine, Trinity Centre for Health Sciences, St. James's  
40 Hospital, Dublin 8, Ireland. E-Mail: gmclaug@tcd.ie or  
41 gavinmclaughlin@research.ait.ie  
42  
43

44  
45 **Running title:** Analytical characterization and pharmacological evaluation of  
46 4-fluoromethylphenidate  
47  
48

49 **Keywords:** New psychoactive substances; psychostimulants;  
50 methylphenidate; 4-fluoromethylphenidate; monoamine transporters; in vitro  
51  
52  
53  
54  
55  
56  
57  
58  
59  
60

## Abstract

Misuse of ( $\pm$ )-*threo*-methylphenidate (methyl-2-phenyl-2-(piperidin-2-yl)acetate; Ritalin<sup>®</sup>, MPH) has long been acknowledged, but the appearance of MPH analogs in the form of 'research chemicals' has only emerged in more recent years. 4-Fluoromethylphenidate (4F-MPH) is one of these recent examples and this study presents the identification and analytical characterization of two powdered 4F-MPH products that were obtained from an online vendor in 2015. Interestingly, the products appeared to have originated from two distinct batches given that one product consisted of ( $\pm$ )-*threo*-4F-MPH isomers whereas the second sample consisted of a mixture of ( $\pm$ )-*threo* and ( $\pm$ )-*erythro* 4F-MPH. Monoamine transporter studies using rat brain synaptosomes revealed that the biological activity of the 4F-MPH mixture resided with the ( $\pm$ )-*threo*- and not the ( $\pm$ )-*erythro* isomers based on higher potencies determined for blockage of dopamine uptake ( $IC_{50}$  4F-MPH<sub>mixture</sub> = 66 nM vs.  $IC_{50}$  ( $\pm$ )-*threo* = 61 nM vs.  $IC_{50}$  ( $\pm$ )-*erythro* = 8,528 nM) and norepinephrine uptake ( $IC_{50}$  4F-MPH<sub>mixture</sub> = 45 nM vs. ( $\pm$ )-*threo* = 31 nM vs.  $IC_{50}$  ( $\pm$ )-*erythro* = 3,779 nM). In comparison, MPH was three times less potent than ( $\pm$ )-*threo*-4F-MPH at the dopamine transporter ( $IC_{50}$  = 131 nM) and around 2.5-times less potent at the norepinephrine transporter ( $IC_{50}$  = 83 nM). Both substances were catecholamine selective with  $IC_{50}$  values of 8,805 nM and >10,000 nM for ( $\pm$ )-*threo*-4F-MPH and MPH at the serotonin transporter. These findings suggest that the psychostimulant properties of ( $\pm$ )-*threo*-4F-MPH might be more potent in humans than MPH.

## Introduction

Methylphenidate (methyl-2-phenyl-2-(piperidin-2-yl)acetate; MPH; Ritalin<sup>®</sup>) is a substituted phenethylamine that was first synthesized in 1944 and subsequently recognized as a psychostimulant (Figure 1).<sup>[1,2]</sup> MPH acts primarily by inhibiting the re-uptake of dopamine and norepinephrine resulting in elevated concentrations of these monoamine neurotransmitters within the synaptic cleft.<sup>[3,4]</sup> MPH is widely used in the treatment of attention deficit hyperactivity disorder (ADHD), as the symptoms of this condition are believed to be associated with suppressed levels of these neurotransmitters.<sup>[5,6]</sup> Originally, it was marketed as a mixture of two racemates, consisting of 80% ( $\pm$ )-*erythro* and 20% ( $\pm$ )-*threo* isomers, but successive studies demonstrated that the pharmacologically active diastereomers are associated with the ( $\pm$ )-*threo* form.<sup>[7-10]</sup> Subsequent studies focused on the separation of the two diastereomers and interconversion of ( $\pm$ )-*erythro* racemate to its ( $\pm$ )-*threo* counterpart. The ( $\pm$ )-*threo* racemate exists as two enantiomers, (+)-*threo*-MPH (2*R*,2'*R*) and (-)-*threo*-MPH (2*S*,2'*S*), and the absolute stereochemistry

1  
2  
3 of the most pharmacologically active enantiomer of MPH ((+)-*threo*) has been  
4 characterized<sup>[11-13]</sup> and developed as a medication to treat ADHD in its own  
5 right.<sup>[14]</sup> There have also been efforts to prepare enantiomerically pure  
6 (2*R*,2'*R*)-(+)-*threo*-MPH.<sup>[7]</sup> *In vivo*, (±)-*threo*-MPH undergoes enantioselective  
7 metabolism, which results in substantial differences in the plasma  
8 concentrations of its isomers, depending on route of administration and  
9 formulation.<sup>[15]</sup> Methylphenidate is listed as a Schedule II substance in the  
10 1971 United Nations Convention on Psychotropic Substances.<sup>[16]</sup> In the  
11 United Kingdom (UK), it is controlled as a Class B substance under the  
12 Misuse of Drugs Act 1971.<sup>[17]</sup> In Ireland, it is controlled as a Schedule 2  
13 substance under the Misuse of Drugs Regulations, 1988.<sup>[18]</sup>

14  
15  
16  
17  
18 Methylphenidate and an array of its analogs form a class of compounds that  
19 are well documented in the patent and scientific literature.<sup>[19-23]</sup> Some studies  
20 have focused on the evaluation of structure-activity relationships whereas  
21 others have studied these analogs for other therapeutic indications, including  
22 cocaine addiction, depression, fatigue-related disorders, cerebral palsy and  
23 fibromyalgia.<sup>[19-23]</sup> However, misuse of methylphenidate has been observed  
24 among recreational drug users, presumably due to its psychostimulant  
25 properties. For example, ingestion/insufflation of methylphenidate is popular  
26 among university students to increase concentration, improve alertness, or  
27 solely for recreational purposes.<sup>[24,25]</sup> In the last decade, several unregulated  
28 substances that are very closely related to methylphenidate have been  
29 launched on the new psychoactive substances (NPS) market. As with the  
30 majority of NPS launched by vendors, many of these methylphenidate  
31 analogs have already been described in the pharmaceutical research  
32 literature. For example, ethylphenidate, 3,4-dichloromethylphenidate (3,4-  
33 CTMP), methylnaphthidate (HDMP-28), isopropylphenidate (IPP/IPPD) and  
34 propylphenidate are methylphenidate analogs that have been detected on the  
35 'research chemicals' market.<sup>[6,26]</sup> In April 2015, the UK government imposed a  
36 temporary drug control order (TCDO) on all these analogs.<sup>[27]</sup> Furthermore,  
37 the sale and supply of substances with psychoactive properties are now  
38 controlled in the UK under the newly introduced New Psychoactive  
39 Substances Act 2016.<sup>[28]</sup> Comprehensive analytical characterizations have  
40 recently been described for 4-methylmethylphenidate, 3,4-CTMP,  
41 ethylphenidate, 3,4-dichloroethylphenidate, *N*-benzyl-ethylphenidate and  
42 ethylnaphthidate (HDEP-28), respectively.<sup>[29]</sup> Recent studies from the UK  
43 associated ethylphenidate use to adverse reactions including deaths.<sup>[30-32]</sup> In  
44 addition, it was reported that injection was a common route of administration,  
45 thus adding the risk of harms associated with this method of administration.  
46 Interestingly, co-ingestion of ethanol and methylphenidate has been reported  
47 to form ethylphenidate *in vivo* by transesterification.<sup>[26,33]</sup> In Ireland, the sale  
48 and supply of analogs of methylphenidate would be controlled under the  
49 Criminal Justice (Psychoactive Substances) Act 2010.<sup>[34]</sup>

1  
2  
3  
4 4-Fluoromethylphenidate (4F-MPH) (Figure 1) is a methylphenidate analog  
5 that was developed within the pharmaceutical setting. However, in November  
6 2015, it was first notified by the European Monitoring Centre for Drugs and  
7 Drug Addiction (EMCDDA) Early Warning System following its detection on  
8 the recreational market.<sup>[35]</sup> Previous *in vitro* studies indicated that the addition  
9 of a fluorine atom to the *para*-position of the phenyl ring in the  
10 methylphenidate parent structure led to slight increases in potency related to  
11 displacement of [<sup>3</sup>H]WIN-35,428 and [<sup>3</sup>H]dopamine uptake inhibition.<sup>[4]</sup>  
12  
13  
14

15  
16 This study describes the analytical characterization of two powdered samples  
17 and a set of tablets of 4-fluoromethylphenidate that were obtained from the  
18 same vendor based in the United Kingdom in 2015. The study was triggered  
19 following the receipt of two powdered 4F-MPH samples from an online  
20 retailer. Various chromatographic, spectroscopic and mass spectrometric  
21 analysis methods were employed, followed by x-ray crystal structure analysis.  
22 One of the vendor samples was found to contain (±)-*threo*-4F-MPH, which  
23 was consistent with the expected racemate based on the current knowledge  
24 of the biological activity of (±)-*threo*-MPH. Unexpectedly, the analysis of the  
25 second sample revealed that it consisted of a mixture of (±)-*threo* and (±)-  
26 *erythro*-4F-MPH. This suggested that the two powdered vendor products  
27 might have originated from different batches. The two racemates were  
28 isolated from the mixture, purified, and converted to HCl salts prior to full  
29 analytical characterization. In addition, 4F-MPH tablets were also obtained  
30 from the same vendor and analysed for the presence of the (±)-*threo* and/or  
31 (±)-*erythro* form.  
32  
33  
34  
35  
36

37  
38 It was hypothesized that the distinct forms of 4F-MPH encountered in these  
39 products would result in different pharmacological properties similar to what  
40 has been reported for MPH, thus, potentially resulting in different effects in  
41 consumers. For this reason, the ability of the test drugs to inhibit uptake of  
42 [<sup>3</sup>H]dopamine, [<sup>3</sup>H]norepinephrine and [<sup>3</sup>H]serotonin was investigated using  
43 synaptosomal preparations from rat brain. The isolated diastereomeric  
44 racemates (±)-*threo* and (±)-*erythro*-4F-MPH, the (±)-*threo*/(±)-*erythro* mixture,  
45 and MPH were included to study the effects at dopamine transporters (DAT),  
46 norepinephrine transporters (NET) and serotonin transporters (SERT),  
47 respectively.  
48  
49  
50

## 51 **Experimental**

### 52 *Chemicals*

53  
54 All reagents and dry solvents used in the syntheses were obtained from  
55 Sigma Aldrich Ltd (Arklow, Co. Wicklow, Ireland). LC-MS grade solvents were  
56  
57  
58  
59  
60

1  
2  
3 obtained from Fisher Scientific (Dublin, Ireland). Preparative silica gel thin  
4 layer chromatography plates (UV<sub>254</sub>, GF 20 x 20 cm, 2000 microns) were  
5 obtained from Analtech (Newark, NJ, USA). Two powdered samples of 4-  
6 fluoromethylphenidate (4F-MPH) and tablets were obtained from an online  
7 vendor based in the UK in 2015.  
8  
9

#### 10 *Isolation of 4-fluoromethylphenidate (4F-MPH) diastereomers*

11  
12  
13 A solution of 4-fluoromethylphenidate (568 mg, vendor sample containing  
14 both diastereomers) in water (15 mL) was made basic with sodium hydroxide  
15 (pH 10-11). This was extracted with dichloromethane (2 x 10 mL). Drying  
16 (anhydrous magnesium sulphate) and removal of the solvent afforded a  
17 colorless oil (355 mg). Preparative TLC (silica gel, 2 mm; mobile phase: ethyl  
18 acetate; extraction solvent: ethanol) afforded two fractions, both colorless  
19 viscous oils (23 and 84 mg). The HCl salts were formed (2M hydrogen  
20 chloride in diethyl ether) and crystallized from ethanol for x-ray  
21 crystallography.  
22  
23  
24  
25

#### 26 *(±)-threo-4F-MPH freebase (bottom band of preparative TLC)*

27  
28 <sup>1</sup>H NMR (CDCl<sub>3</sub>) δ 7.36-7.22 (m; 2H; H-2'/6'), 7.14-6.98 (m; 2H; H-3'/5'), 3.70  
29 (s; 3H; CH<sub>3</sub>), 3.61 (d; *J* = 10.2 Hz; 1H; H-2), 3.25-3.13 (m; 2H; H-2'' and one H  
30 from H-6''), 2.75 (td; *J* = 12.0, 2.9 Hz; 1H; one from H-6''), 1.76-1.69 (m; 1H;  
31 one H from H-4''), 1.66-1.58 (m; 1H; one H from H-5''), 1.46 (dddd; 1H; *J* =  
32 16.1, 12.4, 8.4, 3.8 Hz; one H from H-5''), 1.33 -1.19 (m; 2H; one H each from  
33 H-4'' and H-3'') and 1.08-0.97 (m; 1H; one H from H-3'') ppm; <sup>13</sup>C NMR  
34 (CDCl<sub>3</sub>) δ 173.53 (C=O), 162.24 (d; *J*<sub>CF</sub> = 246.5 Hz; C-4'), 131.98 (C-1'),  
35 130.08 (d; *J*<sub>CF</sub> = 7.8 Hz; C-2'/6'), 115.63 (d; *J*<sub>CF</sub> = 21.5 Hz; C-3'/5'), 59.01 (C-  
36 2''), 57.07 (C-2), 52.32 (CH<sub>3</sub>), 46.69 (C-6''), 29.29 (C-3''), 25.43 (C-5'') and  
37 24.05 (C-4'') ppm; <sup>19</sup>F NMR (CDCl<sub>3</sub>) δ -114.63 ppm.  
38  
39  
40  
41  
42

#### 43 *(±)-threo-4F-MPH hydrochloride*

44  
45 Melting point: 202-204 °C. <sup>1</sup>H NMR (DMSO) δ 7.38-7.32 (m; 2H; H-2'/6'), 7.28-  
46 7.21 (m; 2H; H-3'/5'), 4.12 (d; *J* = 9.6 Hz; 1H; CH; H-2), 3.83-3.75 (m; 1H; CH;  
47 H-2'') 3.32 (s; 3H; CH<sub>3</sub>), 3.28 (apparent d; *J* = 13.1 Hz; 1H; one H from H-6''),  
48 2.96 (apparent t; *J* = 11.6 Hz; 1H; one H from H-6''), 1.74-1.64 (m; 2H; one H  
49 each from H-4'' and 5''), 1.63-1.57 (m; 1H; one H from H-5''), 1.47-1.38 (m;  
50 1H; one H from H-4'') and 1.46-1.27 (m; 2H; H-3'') ppm; <sup>13</sup>C NMR (DMSO) δ  
51 171.48 (C=O), 162.21 (d; *J*<sub>CF</sub> = 244.9 Hz; C-4'), 131.03 (d; *J*<sub>CF</sub> = 8.4 Hz; C-  
52 2'/6'), 130.52 (C-1'), 116.25 (d; *J*<sub>CF</sub> = 21.5 Hz; C-3'/5'), 56.93 (C-2''), 53.05  
53 (CH<sub>3</sub>), 52.68 (C-2), 44.84 (C-6''), 26.03 (C-3''), 21.94 (C-5'') and 21.55 (C-4'')  
54 ppm; <sup>19</sup>F NMR (DMSO) δ -113.87 ppm. HR-APCI-MS observed *m/z*  
55 252.139854 (theory [M + H]<sup>+</sup>: C<sub>14</sub>H<sub>19</sub>FNO<sub>2</sub> *m/z* 252.139433, Δ = 1.7 ppm).  
56  
57  
58  
59  
60

(±)-erythro-4F-MPH freebase (top band of preparative TLC)

$^1\text{H}$  NMR ( $\text{CDCl}_3$ )  $\delta$  7.47-7.34 (m; 2H; H-2'/6'), 7.12-6.99 (m; 2H; H-3'/5'), 3.68 (s; 3H;  $\text{CH}_3$ ), 3.56 (d;  $J = 10.3$  Hz; 1H; H-2), 3.11 (td;  $J = 10.1, 2.2$  Hz; 1H; H-2''), 3.01 (apparent d;  $J = 11.6$  Hz; 1H; one H from H-6''), 2.55 (td;  $J = 11.6, 2.9$  Hz; 1H; one H from H-6''), 1.87-1.68 (m; 2H; one H from H-3'' and H-4''), 1.66-1.58 (m; 1H; one H from H-5'') and 1.55-1.25 (m; 3H; one H each from H-3'', 4'' and 5'') ppm;  $^{13}\text{C}$  NMR ( $\text{CDCl}_3$ )  $\delta$  172.84 (C=O), 162.50 (d;  $J_{\text{CF}} = 246.5$  Hz; C-4'), 131.46 (C-1'), 130.36 (d;  $J_{\text{CF}} = 7.9$  Hz; C-2'/6'), 115.95 (d;  $J_{\text{CF}} = 21.0$  Hz; C-3'/5'), 59.09 (C-2''), 57.04 (C-2), 52.06 ( $\text{CH}_3$ ), 46.94 (C-6''), 30.58 (C-3''), 25.39 (C-5'') and 24.22 (C-4'') ppm;  $^{19}\text{F}$  NMR ( $\text{CDCl}_3$ )  $\delta$  -114.28 ppm.

(±)-erythro-4F-MPH hydrochloride

Melting point: 198-200 °C.  $^1\text{H}$  NMR (DMSO)  $\delta$  ppm 7.51-7.44 (m; 2H; H-2'/6'), 7.32-7.24 (m; 2H; H-3'/5'), 4.11 (d,  $J = 9.4$  Hz; 1H; CH; H-2), 3.70-3.66 (m; 1H; CH; H-2''), 3.65 (s; 3H;  $\text{CH}_3$ ), 3.14 (apparent d,  $J = 13.0$  Hz; 1H; one H from H-6''), 2.83-2.80 (m; 1H; one H from H-6''), 1.91-1.85 (m; 1H; one H from H-3''), 1.82-1.69 (m; 2H; H-4''/H-5''), 1.68-1.59 (m; 2H; one H each from H-4''/H-5'' and H-3'') and 1.55-1.46 (m; 1H; one H from H-4''/H-5'') ppm;  $^{13}\text{C}$  NMR (DMSO)  $\delta$  171.36 (C=O), 162.81 (d;  $J_{\text{CF}} = 244.5$  Hz; C-4'), 131.55 (d;  $J_{\text{CF}} = 8.5$  Hz; C-2'/6'), 129.85 (C-1'), 116.65 (d;  $J_{\text{CF}} = 21.6$  Hz; C-3'/5'), 57.55 (C-2), 53.55 (C-2''), 53.00 ( $\text{CH}_3$ ), 45.26 (C-6''), 27.39 (C-3''), 22.10 (C-5'') and 21.93 (C-4'') ppm;  $^{19}\text{F}$  NMR (DMSO)  $\delta$  -113.80 ppm. HR-APCI-MS observed  $m/z$  252.139659 (theory  $[\text{M} + \text{H}]^+$ :  $\text{C}_{14}\text{H}_{19}\text{FNO}_2$   $m/z$  252.139433,  $\Delta = 0.9$  ppm).

## Instrumentation

### Gas chromatography-mass spectrometry (GC-MS)

Samples were prepared to give a 1 mg/mL solution in methanol and analyzed on an Agilent 6890N GC coupled to 5975 Mass Selective Detector (Agilent, Little Island, Cork, Ireland). A HP-ULTRA 1 column (12 m  $\times$  0.2 mm  $\times$  0.33  $\mu\text{m}$ ) was used with helium carrier gas at a constant flow of 1 mL/min and a split ratio of 1:1. The injector was set at 250 °C and the transfer line at 280 °C. The initial oven temperature was 50 °C, held for 2 min, then ramped at 10 °C/min to 100 °C with no hold time. The oven temperature was further ramped at 5 °C/min to 200 °C and then finally ramped at 20 °C/min to 295 °C with a hold time of 1 min. The mass spectra were collected after a 4.0 min solvent delay time. The ionization energy was set at 70 eV and the mass range was  $m/z$  40-550. The total run time was 32.75 min.

### *Liquid chromatography-mass spectrometry (LC-MS)*

LC-MS analyses were performed on an Agilent 1100 HPLC system equipped with a G13795 degasser, G1312A BinPump, a G1313A ALS and G1316A column oven (COLCOM) (Agilent, Little Island, Cork). Separation was obtained on an Allure PFP Propyl column (5  $\mu\text{m}$ , 50 x 2.1 mm) Restek (Bellefonte, PA, USA). Mobile phase A consisted of 0.1% formic acid in water, whereas, mobile phase B consisted of 0.1% formic acid in acetonitrile. The Agilent LC-MSD settings were as follows: positive electrospray mode, capillary voltage 3500 V, drying gas ( $\text{N}_2$ ) 12 L/min at 350  $^\circ\text{C}$ , nebulizer gas ( $\text{N}_2$ ) pressure 50 psi, SIM  $m/z$  252 and scan mode  $m/z$  70-500, fragmentor voltage 50 and 110 V. Samples for LC-MS analysis were dissolved in acetonitrile/water (1:1, containing 0.1% formic acid) at a concentration of 10  $\mu\text{g}/\text{mL}$ . The injection volume was 5.0 and 10.0  $\mu\text{L}$ , flow rate was 0.8 mL/min and the column temperature was 30  $^\circ\text{C}$ . Total run time was 25 min. The following gradient elution program was used: 0-2 min 2% B, followed by an increase to 60% B within 15 min, followed by another increase to 80% B within 18 min before returning to 2% B within 25 min.

### *High resolution mass spectrometry (HR-MS)*

APCI experiments were carried out on a Bruker micrOTOF-Q III spectrometer interfaced to a Dionex UltiMate 3000 LC. The Agilent tuning mix APCI-TOF was used for mass calibration. Masses were recorded over a range of  $m/z$  100-1600. Operating conditions were as follows: capillary voltage 4000 V, corona 4000 nA, nebulizer gas 2.0 bar, drying gas flow rate 3.0 L/min, drying gas temperature 100-200  $^\circ\text{C}$ , vaporizer temperature 100-400  $^\circ\text{C}$ . MicroTof control and HyStar software were used for data analysis.

### *Nuclear magnetic resonance spectroscopy (NMR)*

The free base samples were prepared in deuterated chloroform ( $\text{CDCl}_3$ ) at a concentration of 20 mg/mL. The hydrochloride salt samples were prepared in deuterated dimethyl sulfoxide ( $\text{DMSO}-d_6$ ) at a concentration of 20 mg/mL.  $^1\text{H}$  (600 MHz) and  $^{13}\text{C}$  (150 MHz) spectra were recorded on a Bruker AV600 NMR spectrometer using a 5 mm TCI cryoprobe.  $^1\text{H}$  NMR spectra were referenced to an external TMS reference at  $\delta = 0$  ppm.  $^{19}\text{F}$  (376 MHz) spectra were recorded on a Bruker DPX400 NMR spectrometer and the external reference was trifluorotoluene set at  $\delta = -64$  ppm.

### *X-ray crystallography*

Data for samples ( $\pm$ )-*erythro* and ( $\pm$ )-*threo*-4F-MPH were collected on a Bruker APEX DUO using Cu K $\alpha$  radiation ( $\lambda = 1.54178$   $\text{\AA}$ ) at 100(2) K (Oxford

Cobra Cryosystem) with a Mitegen holder. Bruker APEX<sup>[36]</sup> software was used to collect and reduce data, determine the space group. XT<sup>[37]</sup> was used to solve and XL<sup>[38]</sup> in OLEX 2<sup>[39]</sup> refine the structure. Absorption corrections were applied using SADABS 2014.<sup>[40]</sup> All non-hydrogen atoms were refined anisotropically. Hydrogen atoms were assigned to calculated positions using a riding model with appropriately fixed isotropic thermal parameters. N-H hydrogens were located and refined with restraints and with the  $U_{\text{iso}} = 1.2U_{\text{eq}}$  of the carrier atom in both structures. In the *threo*-4F-MPH structure, the fluorophenyl ring was disordered in two positions with occupancies of 85/15%. Restraints were used in the model (DFIX, RIGU, SADI).

Crystal Data for ( $\pm$ )-*erythro*-4F-MPH,  $\text{C}_{14}\text{H}_{19}\text{NO}_2\text{FCl}$  ( $M = 287.75$  g/mol): monoclinic, space group  $P2_1/n$  (no. 14),  $a = 10.4556(5)$  Å,  $b = 8.5173(4)$  Å,  $c = 15.7304(7)$  Å,  $\beta = 90.6392(15)^\circ$ ,  $V = 1400.76(11)$  Å<sup>3</sup>,  $Z = 4$ ,  $T = 100.0$  K,  $\mu(\text{CuK}\alpha) = 2.510$  mm<sup>-1</sup>,  $D_{\text{calc}} = 1.364$  g/cm<sup>3</sup>, 18265 reflections measured ( $10.106^\circ \leq 2\theta \leq 137.044^\circ$ ), 2577 unique ( $R_{\text{int}} = 0.0376$ ,  $R_{\text{sigma}} = 0.0232$ ) which were used in all calculations. The final  $*R_1$  was 0.0355 ( $I > 2\sigma(I)$ ) and  $wR_2$  was 0.1108 (all data). CCDC No. 1503223.

Crystal Data for ( $\pm$ )-*threo*-4F-MPH,  $\text{C}_{14}\text{H}_{19}\text{ClFNO}_2$  ( $M = 287.75$  g/mol): monoclinic, space group  $P2_1/n$  (no. 14),  $a = 11.289(3)$  Å,  $b = 7.2232(16)$  Å,  $c = 18.494(5)$  Å,  $\beta = 106.169(7)^\circ$ ,  $V = 1448.4(6)$  Å<sup>3</sup>,  $Z = 4$ ,  $T = 100(2)$  K,  $\mu(\text{CuK}\alpha) = 2.428$  mm<sup>-1</sup>,  $D_{\text{calc}} = 1.320$  g/cm<sup>3</sup>, 20393 reflections measured ( $8.286^\circ \leq 2\theta \leq 136.614^\circ$ ), 2656 unique ( $R_{\text{int}} = 0.0813$ ,  $R_{\text{sigma}} = 0.0513$ ) which were used in all calculations. The final  $*R_1$  was 0.0525 ( $I > 2\sigma(I)$ ) and  $wR_2$  was 0.1357 (all data). CCDC No. 1503224.  $*R_1 = \frac{\sum ||F_o| - |F_c||}{\sum |F_o|}$ ,  $wR_2 = \left[ \frac{\sum w(F_o^2 - F_c^2)^2}{\sum w(F_o^2)^2} \right]^{1/2}$ .

### Infrared Spectroscopy

IR spectra were recorded on a Perkin Elmer Spectrum 100 FT-IR with Universal ATR sampling accessory (Perkin Elmer, Waltham, MA, USA). The wavelength resolution was set to 2 cm<sup>-1</sup>. IR spectra were collected in a range of 650 - 4000 cm<sup>-1</sup> with 16 scans per spectrum. The IR data were processed using Spectrum Perkin Elmer Version 6.3.4 Software (Perkin Elmer, Waltham, MA, USA).

### Monoamine transporter assays

Male Sprague-Dawley rats (250-300 g, Charles River Laboratories, Wilmington, MA, USA) were housed 2 per cage and maintained on a 12 h light-dark cycle. Food and water were provided ad libitum. Animal use procedures were conducted in accordance with the NIH Guide for the Care and Use of Laboratory Animals, and the Animal Care and Use Committee of



1  
2  
3 the Intramural Research Program of the National Institute on Drug Abuse  
4 (Baltimore, MD, USA). Rats were euthanized by CO<sub>2</sub> narcosis and brains  
5 were processed to yield synaptosomes as previously described.<sup>[41,42]</sup> For  
6 uptake assays, synaptosomes were incubated with different concentrations of  
7 the test drugs in the presence of 5 nM [<sup>3</sup>H]dopamine, 10 nM  
8 [<sup>3</sup>H]norepinephrine, or 5 nM [<sup>3</sup>H]serotonin. The uptake assays were  
9 terminated by vacuum filtration and retained radioactivity was quantified by  
10 scintillation counting.  
11  
12  
13

## 14 15 16 Results and Discussion

17  
18 Manufacturers and entrepreneurs dedicated to the commercial exploration of  
19 'research chemicals' destined for recreational drug markets, are utilizing the  
20 scientific and patent literature to generate ideas for launching new  
21 compounds. Since methylphenidate and a series of its analogs have been  
22 well documented in the literature, e.g.<sup>[19-23]</sup>, it was not surprising to see that  
23 several methylphenidate-based NPS have also been encountered on the  
24 'research chemicals' market. One of the more recent methylphenidate-based  
25 NPS was 4-fluoromethylphenidate (4F-MPH). 4F-MPH is one of the  
26 methylphenidate analogs described in the literature in studies evaluating ring  
27 substituted methylphenidate analogs as potential therapeutics for cocaine  
28 addiction and fibromyalgia.<sup>[19-21]</sup> 4F-MPH did not appear to have a history of  
29 human usage prior to its distribution online through vendors of 'research  
30 chemicals'.  
31  
32  
33  
34  
35

36  
37 In this study, two powdered samples and a set of tablets were obtained from  
38 the same vendor based in the United Kingdom in 2015. Initially, it was noticed  
39 that the two powdered products showed different solubility in solvents such as  
40 methanol and water. As the analyses progressed, it was noticed that one  
41 product contained the *threo*-racemate, whereas the other included a second  
42 compound suspected to represent a diastereomeric form based on similar  
43 mass spectra. Analysis by gas chromatography-mass spectrometry (GC-MS)  
44 suggested that this was the case and it was hypothesized that this product  
45 was most likely the racemic *erythro*- form of 4F-MPH. In order to investigate  
46 further, the 4F-MPH sample containing both diastereomers was dissolved in  
47 water and made alkaline with sodium hydroxide. This was extracted with  
48 dichloromethane, dried with anhydrous magnesium sulphate, followed by  
49 solvent removal to afford a colorless oil. Preparative thin-layer  
50 chromatography (TLC) afforded two fractions as colorless viscous oils. The  
51 hydrochloride salts were formed (2M hydrogen chloride in diethyl ether),  
52 crystallized from ethanol and subjected to extensive analytical  
53 characterization.  
54  
55  
56  
57  
58  
59  
60

1  
2  
3  
4 From examination of the methylphenidate synthesis literature, it seemed  
5 plausible that the presence of the *erythro*-racemate might have reflected a  
6 lack of purification at the end of the synthesis procedure. For example, one  
7 synthesis procedure employed for a range of methylphenidate analogs<sup>[4]</sup>  
8 involved the reaction of 2-phenylacetonitrile and 2-bromopyridine with  
9 potassium *tert.*-butoxide in tetrahydrofuran (THF). This led to the formation of  
10 a nitrile intermediate and a ketone by-product, which could be easily removed  
11 in the subsequent steps. The nitrile intermediate was hydrolysed under acidic  
12 conditions leading to the formation of an acetamide species. Hydrogenation of  
13 the pyridine ring to piperidine followed, leading to the formation of two racemic  
14 *erythro*- and *threo* acetamide intermediates. At this stage, the *erythro* species  
15 was present at a higher ratio compared to the *threo*-species. This mixture was  
16 then hydrolysed to form *erythro*- and *threo*-acetic acid entities. An  
17 epimerization process with potassium hydroxide flipped these ratios leading to  
18 a larger percentage of the *threo*-acetic acid intermediate. Esterification with  
19 methanol leads to the formation of the final *threo/erythro* acetate species,  
20 which was then purified by recrystallization to isolate the ( $\pm$ )-*threo*-racemate.<sup>[4]</sup>  
21 From this perspective, and provided a similar synthetic route was used by the  
22 manufacturers, failure to isolate the ( $\pm$ )-*threo*-racemate by appropriate  
23 recrystallization might have resulted in the presence of both racemates in the  
24 final product. An alternative explanation might be that the manufacturers  
25 decided to skip the recrystallization step on purpose.

### 33 Analytical Features

#### 36 Gas chromatography mass spectrometry

37  
38 The gas chromatographic method used was able to achieve satisfactory  
39 separation between the ( $\pm$ )-*threo*- (18.13 min) and ( $\pm$ )-*erythro*- racemates  
40 (18.04 min) (Figure 2). The EI mass spectra obtained for both racemates were  
41 identical. The base peak was observed at  $m/z$  84 and it is suggested that this  
42 was due to the formation of a tetrahydropyridinium species ( $C_5H_{10}N^+$ ),  
43 following the loss of a methyl 4-fluorophenylacetate moiety from the molecular  
44 ion. This fragment was consistent with the EI mass spectral data for  
45 methylphenidate, ethylphenidate and 4F-MPH available in the literature.<sup>[26,43-  
46] The fragment observed at  $m/z$  190 was consistent with the formation of a  
47 4-fluorophenyl(piperidin-2-ylidene)methyl cation species ( $C_{12}H_{13}FN^+$ ). The  
48 detection of  $m/z$  168 may be rationalized by the loss of the tetrahydropyridine  
49 moiety from the parent structure, which gave rise to a radical cation and  
50 formation of a methyl fluorophenylacetate species ( $C_9H_8FO_2^{+\cdot}$ ). This fragment  
51 was also consistent with the EI-MS data for methylphenidate and  
52 ethylphenidate.<sup>[26,43-44]</sup> However, in the case of methylphenidate and  
53 ethylphenidate, this ion would be encountered at  $m/z$  150 (methyl  
54  
55  
56  
57  
58  
59  
60</sup>

1  
2  
3 phenylacetate moiety) and  $m/z$  164 (ethyl phenylacetate moiety), respectively.  
4 The fragment at  $m/z$  109 can be described by the formation of a tropylium ion,  
5 consistent with the formation of tropylium ion reported in the EI-MS of  
6 methylphenidate and ethylphenidate at  $m/z$  91. The fragment at  $m/z$  56 could  
7 represent the formation of a dihydroazetium ion. During GC analysis, a  
8 second product at 7.26 min was also observed in the chromatogram  
9 (Supporting Information) and it was believed that this product might have  
10 been a degradant resulting from the thermal decomposition of 4F-MPH within  
11 the GC system. This GC-induced reaction was thought to involve the loss of  
12 the tetrahydropyridine moiety and the formation of an enol tautomer of methyl  
13 4-fluorophenylacetate, which subsequently tautomerized to methyl 4-  
14 fluorophenyl acetate. Interestingly, the formation of the GC-induced product,  
15 methyl 4-fluorophenyl acetate, was found to be slightly higher (53.6 %) in the  
16 chromatogram of the ( $\pm$ )-*threo*- 4FMPH racemate, compared to that of the ( $\pm$ )-  
17 *erythro*- 4FMPH racemate (43.7%). This type of degradation was consistent  
18 with literature reports on methylphenidate and its analogs<sup>[29,47-48]</sup>, however,  
19 the suggested identity remains tentative as a reference standard was not  
20 available.  
21  
22  
23  
24  
25

#### 26 27 *Liquid chromatography-mass spectrometry*

28  
29  
30 Analysis of both ( $\pm$ )-*threo*- and ( $\pm$ )-*erythro*- racemates of 4F-MPH using high  
31 performance liquid chromatography (HPLC) confirmed satisfactory separation  
32 for identification purposes. A retention time of 8.90 min was obtained for the  
33 ( $\pm$ )-*erythro* form, whereas a retention time of 9.81 min was obtained for the  
34 ( $\pm$ )-*threo* racemate (Figure 3). The electrospray ionization (ESI) single  
35 quadrupole mass spectra obtained from in-source collision-induced  
36 dissociation (CID) (fragmentor 110 V) of the 4F-MPH racemates shared two  
37 key ions. The suggested pathways are shown in Figure 3. In the mass spectra  
38 of both racemates, the fragment observed at  $m/z$  252 represented the  
39 protonated molecule with 100% relative abundance. The product ion observed  
40 at  $m/z$  84 might have represented a loss of the methyl 4-fluorophenylacetate  
41 moiety from the protonated molecule resulting in the formation of a  
42 tetrahydropyridinium species ( $C_5H_{10}N^+$ ) and this was also present at  
43 approximately 95% abundance.  
44  
45  
46  
47  
48

#### 49 *Nuclear magnetic resonance spectroscopy (NMR)*

50  
51 The chemical structures of the ( $\pm$ )-*threo*- and ( $\pm$ )-*erythro*- 4F-MPH racemates  
52 and powdered vendor samples were elucidated using both one-dimensional  
53 and two-dimensional NMR experiments (Figure 4, Supporting Information).  
54 The NMR spectra associated with the 4F-MPH HCl salt forms of the ( $\pm$ )-  
55 *erythro*- and ( $\pm$ )-*threo*- racemates shared similar characteristics but significant  
56 differences could also be observed between some of the proton and carbon  
57  
58  
59  
60

1  
2  
3 chemical shifts that facilitated differentiation between the racemates. For  
4 example, in the  $^1\text{H}$  spectrum of the ( $\pm$ )-*erythro*- racemate, the signals  
5 associated with the protons on the aromatic ring were observed as multiplets  
6 between 7.51-7.44 and 7.32-7.24 ppm. However, in the spectrum of the ( $\pm$ )-  
7 *threo*- counterpart these proton resonances were shifted upfield to 7.38-7.32  
8 and 7.28-7.21 ppm, respectively. Furthermore, the proton signal for the methyl  
9 group of the ( $\pm$ )-*threo*- racemate was shifted upfield (3.32 ppm) compared to  
10 the same signal associated with the ( $\pm$ )-*erythro* racemate (3.65 ppm). The  
11 proton environment around the piperidine ring provided further distinguishing  
12 features. For example, in the  $^1\text{H}$  spectrum of the ( $\pm$ )-*erythro*- racemate, the  
13 proton signals associated with H-2'' were observed as a multiplet between  
14 3.70-3.66 ppm. The same proton resonances in the ( $\pm$ )-*threo*- counterpart  
15 were also observed as a multiplet but were shifted downfield to 3.83-3.75  
16 ppm. Moreover, one proton associated with H-6'' was observed as a doublet  
17 at 3.14 ppm in the proton spectrum of ( $\pm$ )-*erythro*- 4F-MPH. In comparison,  
18 the same proton signal in the ( $\pm$ )-*threo*- counterpart was shifted downfield and  
19 observed at 3.28 ppm (Figure 4). The second proton associated with H-6''  
20 also provided a distinguishing feature as it appeared as a triplet at 2.96 ppm  
21 in the ( $\pm$ )-*threo*- spectrum. However, the same proton signal in the ( $\pm$ )-*erythro*-  
22 counterpart was observed as a multiplet between 2.83-2.80 ppm.  
23  
24  
25  
26  
27  
28  
29

30 Some distinguishing features were also observed in the  $^{13}\text{C}$  NMR spectra  
31 (Supporting Information). For example, the  $^{13}\text{C}$  spectrum of the ( $\pm$ )-*erythro*-  
32 racemate revealed the carbonyl chemical shift at 171.36 ppm, whereas the  
33 same signal was observed at 171.48 ppm in the spectrum of the ( $\pm$ )-*threo*-  
34 counterpart. The aromatic region also provided distinct differences. In the  
35 spectrum of the ( $\pm$ )-*erythro*- racemate, the aromatic carbon signals (C-2'/6', C-  
36 3'/5') were observed at 131.55 and 116.65 ppm. In the spectrum of the ( $\pm$ )-  
37 *threo*- racemate, the same carbon signals were shifted upfield to 131.03 and  
38 116.21 ppm, respectively. However, another aromatic carbon signal (C-1')  
39 was observed at 129.85 ppm in the ( $\pm$ )-*erythro*- spectrum, whereas the same  
40 carbon signal was shifted downfield and observed at 130.52 ppm in the ( $\pm$ )-  
41 *threo*- spectrum. Moreover, the carbon of the methine group (C-2) was  
42 observed at 57.55 ppm in the spectrum of the ( $\pm$ )-*erythro*- racemate, which  
43 shifted upfield in the ( $\pm$ )-*threo*- counterpart and observed at 52.68 ppm. The  
44 piperidine carbon (C-2'') was observed at 53.55 ppm in the spectrum of the  
45 ( $\pm$ )-*erythro*- racemate, which shifted downfield in the ( $\pm$ )-*threo*- counterpart  
46 and observed at 56.93 ppm. In general, all carbon signals associated with the  
47 piperidine ring (44.84, 26.03, 21.94 and 21.55 ppm) were shifted upfield in the  
48 ( $\pm$ )-*threo*- spectrum compared to the same signals in the ( $\pm$ )-*erythro*- spectrum  
49 (45.26, 27.39, 22.10 and 21.93 ppm). The mixture contained the  
50 characteristics of both racemates.  
51  
52  
53  
54  
55  
56  
57  
58  
59  
60

### X-Ray crystallography

Both salts were crystallized from a water/ethanol mixture to give colorless needle shaped crystals. The crystal structures of both diastereomers are shown in Figures 5A and 5B. Both crystallized in the monoclinic space group  $P2(1)/n$  as the chloride salt. The ( $\pm$ )-*erythro* salt is shown as the (*R,S*)-enantiomer (C2, C3) and the ( $\pm$ )-*threo* as the (*S,S*) enantiomer. As these molecules crystallized in a centrosymmetric space group, the inverse enantiomer was also equally present. The piperidine ring in both compounds was in the chair conformation. In both diastereomers, the piperidine was substituted in an equatorial position. The plane of piperidine ring to the fluorophenyl ring was  $69.9^\circ$  in the *erythro* and almost orthogonal at  $84.5^\circ$  in the *threo* salt. Each  $\text{NH}_2$  group was involved in hydrogen bonding. In the *erythro* salt the  $\text{Cl}^-$  anion was strongly hydrogen bound to two  $\text{NH}_2$  groups ( $\text{N1}\dots\text{Cl1}$ ,  $3.0704(12)\text{\AA}$ ,  $170.1(15)^\circ$ ;  $\text{N1}\dots\text{Cl1}^{\#4}$ ,  $3.2414(12)\text{\AA}$ ,  $146.8(16)^\circ$ , symmetry transformation  $\#4 = 1-x, 1-y, 1-z$ ) with the carbonyl oxygen more loosely held by weak C-H interactions ( $\text{C3}\dots\text{O1}^{\#1}$ ,  $3.3239(17)\text{\AA}$ ,  $150^\circ$ , symmetry transformation  $\#1 = -x, 1-y, 1-z$ ). This formed a symmetric dimer (Supporting Information). The *threo* salt also displayed  $\text{NH}\dots\text{Cl}$  interactions ( $\text{N1}\dots\text{Cl1}$   $3.134(2)\text{\AA}$ ,  $167(3)^\circ$ ;  $\text{N1}\dots\text{Cl1}^{\#1}$   $3.215(2)\text{\AA}$ ,  $164(2)^\circ$ , symmetry transformation  $\#1 = 3/2-x, 1/2+y, -1/2-z$ ). However, N1 formed a bifurcated hydrogen bond to the carbonyl oxygen ( $\text{N1}\dots\text{O1}^{\#1}$   $3.011(3)\text{\AA}$ ,  $113(2)^\circ$ ). Unlike the *erythro* salt, the *threo* salt formed an extended ribbon parallel to the *b* – axis (Supporting Information) These structural motifs are also seen in similar congeners which also form hydrogen bonded dimers or ribbons extending parallel to the *b*-axis.<sup>[49]</sup>

### Infrared spectroscopy

The ( $\pm$ )-*threo*- and ( $\pm$ )-*erythro*- racemates of 4F-MPH were also subjected to analysis by infrared (IR) spectroscopy. The IR spectra associated with the 4F-MPH HCl salt forms of the ( $\pm$ )-*erythro*- and ( $\pm$ )-*threo*- racemates shared similar characteristics although one difference was observed that facilitated differentiation (Supporting Information). The absorbance for the carbonyl group was observed at  $1743\text{ cm}^{-1}$  for the ( $\pm$ )-*threo*- racemate compared to  $1726\text{ cm}^{-1}$  for the ( $\pm$ )-*erythro*- racemate. The vendor sample consisting of both racemates contained two carbonyl absorbance values consistent with those of the isolated ( $\pm$ )-*erythro*- and ( $\pm$ )-*threo*- 4FMPH racemates. The second powdered vendor sample and the tablet shared the same characteristics as those of the ( $\pm$ )-*threo*- 4FMPH racemate. It was encouraging to observe that the infrared spectroscopic analysis was able to provide an important distinguishing feature between the 4F-MPH racemates, which would be beneficial when working within a forensic science laboratory setting.

### Monoamine transporter activity

When the analytical investigation revealed that two distinct 4F-MPH products were present, further questions arose about the potential for distinct pharmacological properties associated with the individual ( $\pm$ )-*threo*- and ( $\pm$ )-*erythro*-form of 4F-MPH. Figure 6 shows the effects of the ( $\pm$ )-*threo/erythro* mixture, ( $\pm$ )-*threo*-4F-MPH, ( $\pm$ )-*erythro*-4F-MPH and methylphenidate (MPH) on the uptake of [ $^3$ H]dopamine (DA), [ $^3$ H]norepinephrine (NE) and [ $^3$ H]serotonin (5-HT) by their respective transporters DAT, NET and SERT (Figure 6A-6D). The corresponding IC<sub>50</sub> values for inhibition of uptake are provided in Table 1 and MPH was included for comparison. As revealed from the dose response curves, all test drugs were fully effective uptake inhibitors at DAT and NET, with little activity at SERT, thus, displaying catecholamine selectivity.

The 4F-MPH mixture was about twice as potent as MPH at DAT and NET, although addition of the fluorine atom to the 4-position of the phenyl ring did not increase potency at SERT. Importantly, the data shown in Table 1 indicate that the biological activity of the 4F-MPH mixture predominantly resided with the ( $\pm$ )-*threo*- and not the ( $\pm$ )-*erythro* isomers given that higher potencies were determined for dopamine uptake (IC<sub>50</sub> *threo* = 61 nM vs. IC<sub>50</sub> *erythro* = 8,528 nM) and norepinephrine uptake (IC<sub>50</sub> *threo* = 31 nM vs. IC<sub>50</sub> *erythro* = 3,779 nM) at DAT and NET, respectively. The reduced activity of ( $\pm$ )-*erythro* isomers at DAT has been reported previously on other ring-substituted analogs.<sup>[4]</sup> Previous investigations also demonstrated that ( $\pm$ )-*threo*-4F-MPH showed nanomolar binding affinity toward DAT (IC<sub>50</sub> = 35 nM, [ $^3$ H]WIN-35,428) and that it inhibited [ $^3$ H]dopamine uptake via DAT in rat brain synaptosomal preparations (IC<sub>50</sub> = 142 nM)<sup>[4]</sup> consistent with the findings reported in this study. Consistent with the data shown in Table 1, ( $\pm$ )-*threo*-4F-MPH did not show any appreciable binding affinity at SERT (IC<sub>50</sub> > 10  $\mu$ M, [ $^3$ H]citalopram). Furthermore, ( $\pm$ )-*threo*-4F-MPH was shown to be about three times more potent than MPH in a drug discrimination assay.<sup>[50]</sup> Overall, it appears that the acetate group and the piperidine ring must be oriented in the opposite direction for the drugs to interact optimally with transporter proteins.

### Conclusion

The analytical characterization of two 4F-MPH powders obtained from the same vendor of 'research chemicals' revealed the presence of ( $\pm$ )-*threo* isomers in one and a mixture of ( $\pm$ )-*threo* / ( $\pm$ )-*erythro*-4F-MPH racemates in the other, which suggested a failure to isolate the ( $\pm$ )-*threo*-racemate that may have formed during the synthesis procedure of the main ( $\pm$ )-*threo* product. Various chromatographic, spectroscopic and mass spectrometric platforms were employed followed by x-ray crystal structure analysis. ( $\pm$ )-*threo*-4F-MPH

1  
2  
3 was shown to be more potent than methylphenidate in its ability to inhibit  
4 uptake of [<sup>3</sup>H]dopamine and [<sup>3</sup>H]norepinephrine into rat brain synaptosomes,  
5 with significantly less activity associated with inhibition of the serotonin  
6 transporter. The significantly reduced potency of (±)-*erythro*-4F-MPH was  
7 consistent with (±)-*erythro*-MPH and other (±)-*erythro*-MPH analogs reported  
8 in the literature. These findings suggest that the psychostimulant properties of  
9 (±)-*threo*-4F-MPH might be more potent in humans than MPH. Since the  
10 biological activity resides in the (±)-*threo* form, it is anticipated that other  
11 MPH-derived 'research chemicals' on the market might also display this  
12 configuration.  
13  
14  
15  
16

### 17 Acknowledgements

18 The authors thank Scientific Supplies Ltd. (London, UK) for support.  
19  
20  
21  
22

### 23 References

- 24  
25  
26  
27 [1] L. Panizzon. La preparazione di piridil- e piperidil-arilacetoni-trili e di  
28 alcuni prodotti di trasformazione (Parte I). *Helv. Chim. Acta* **1946**, 29,  
29 324.  
30  
31 [2] R. Meier, F. Gross, J. Tripod. Ritalin, eine neuartige synthetische  
32 Verbindung mit spezifischer zentralerregender Wirkungskomponente.  
33 *Klin. Wochenschr.* **1954**, 32, 445.  
34  
35 [3] M. Stahl, *Stahl's Essential Psychopharmacology: Neuroscientific Basis*  
36 *and Practical Applications, 4th edition*, Cambridge University Press,  
37 Cambridge, UK, **2013**.  
38  
39 [4] H.M. Deutsch, Q. Shi, E. Gruszecka-Kowalik, M.M. Schweri. Synthesis  
40 and pharmacology of potential cocaine antagonists. 2. Structure-  
41 activity relationship studies of aromatic ring-substituted  
42 methylphenidate analogs. *J. Med. Chem.* **1996**, 39, 1201.  
43  
44 [5] R.C. Malenka, E.J. Nestler, S.E. Hyman. Chapter 6: Widely Projecting  
45 Systems: Monoamines, Acetylcholine, Orexin. In: *Molecular*  
46 *Neuropharmacology: A Foundation of Clinical Neuroscience* (Eds: A.  
47 Sydor, R.Y. Brown), 2<sup>nd</sup> edition, McGraw-Hill Medical, New York, **2009**.  
48  
49 [6] Advisory Council on the Misuse of Drugs (ACMD). Methylphenidate-  
50 based NPS: A review of the evidence of use and harm. **2015**. Available  
51 at:  
52 [https://www.gov.uk/government/uploads/system/uploads/attachment\\_d](https://www.gov.uk/government/uploads/system/uploads/attachment_data/file/420983/TCDO_methylphenidate_NPS.pdf)  
53 [ata/file/420983/TCDO\\_methylphenidate\\_NPS.pdf](https://www.gov.uk/government/uploads/system/uploads/attachment_data/file/420983/TCDO_methylphenidate_NPS.pdf) [08 August 2016].  
54  
55 [7] M. Prashad. Approaches to the preparation of enantiomerically pure  
56 (2*R*,2'*R*)-(+)-*threo*-methylphenidate hydrochloride. *Adv. Synth. Catal.*  
57 **2001**, 343, 379.  
58  
59  
60

- 1  
2  
3 [8] M. Hartmann, L. Panizzon. Pyridine and piperidine compounds and  
4 process of making same. Patent No. 2507631. CIBA Pharmaceutical  
5 Products Inc. New Jersey, USA, **1950**.  
6  
7 [9] R. Rometsch. Process for the conversion of stereoisomers. Patent No.  
8 US2838519A. CIBA Pharmaceutical Products Inc. New Jersey, USA,  
9 **1958**.  
10 [10] R. Rometsch. Process for the conversion of stereoisomers. Patent No.  
11 Process for the conversion of stereoisomers US 2957880A. CIBA  
12 Pharmaceutical Products Inc. New Jersey, USA, **1960**.  
13 [11] Weisz, A. Dudás. Über stereoisomere 2-Piperidylphenylessigsäure-  
14 methylester. Die Raumstruktur eines 7-Phenyl-aza-  
15 bicyclo[0.2.4]octans. *Monatsh. Chem.* **1960**, *91*, 840.  
16 [12] A. Shafi'ee, S. Marathe, R. Bhatkar, G. Hite. Absolute configurations of  
17 the enantiomeric pheniramines, methylphenidates, and pipradrols. *J.*  
18 *Pharm. Sci.* **1967**, *56*, 1689.  
19 [13] A. Shafi'ee, G. Hite. The absolute configurations of the pheniramines,  
20 methyl phenidates, and pipradrols. *J. Med. Chem.* **1969**, *12*, 266.  
21 [14] M.D. Moen, S.J. Keam. Dexmethylphenidate extended release. A  
22 review of its use in the treatment of attention-deficit hyperactivity  
23 disorder. *CNS Drugs* **2009**, *23*, 1057.  
24 [15] D.J. Heal, D.M. Pierce. Methylphenidate and its isomers - Their role in  
25 the treatment of attention-deficit hyperactivity disorder using a  
26 transdermal delivery system. *CNS Drugs* **2006**, *20*, 713.  
27 [16] United Nations Convention on Psychotropic Substances, 1971.  
28 Available at [https://www.unodc.org/pdf/convention\\_1971\\_en.pdf](https://www.unodc.org/pdf/convention_1971_en.pdf) [7  
29 September 2016].  
30 [17] The Misuse of Drugs Act 1971. Schedule 2. Part II - Class B Drugs.  
31 Available at: <http://www.legislation.gov.uk/ukpga/1971/38/schedule/2> [7  
32 September 2016].  
33 [18] Irish Statue Book. Misuse of Drugs Regulations, 1988. S.I. No.  
34 328/1988. Available at  
35 <http://www.irishstatutebook.ie/eli/1988/si/328/made/en/print> [7  
36 September 2016].  
37 [19] H.M. Deutsch, M.M. Schweri, C.T. Culbertson, L.H. Zalkow. Synthesis  
38 and pharmacology of irreversible affinity labels as potential cocaine  
39 antagonists - aryl 1,4-dialkylpiperazines related to GBR-12783. *Eur. J.*  
40 *Pharmacol.* **1992**, *220*, 173.  
41 [20] M. Froimowitz, C.J. Kelley. Methylphenidate analogs and methods use  
42 thereof. Patent No. WO200/6047330 A9, USA, **2006**.  
43 [21] R.S. Katz, F. Leavitt. Methods for treating fibromyalgia. Patent No.  
44 US2014/0121193 A1, USA. **2014**.  
45 [22] H.M.L. Davies, D.W. Hopper, T. Hansen, Q.X. Liu, S.R. Childers.  
46 Synthesis of methylphenidate analogues and their binding affinities at  
47  
48  
49  
50  
51  
52  
53  
54  
55  
56  
57  
58  
59  
60



- dopamine and serotonin transport sites. *Bioorg. Med. Chem. Lett.* **2004**, *14*, 1799.
- [23] J.S. Markowitz, K.S. Patrick, H.J. Zhu. Isopropylphenidate for the treatment of attention-deficit/hyperactivity disorder and fatigue-related disorders and conditions. Patent No. WO2011/011528 A1. Musc Foundation for Research Development, Charleston, SC, USA, **2011**.
- [24] S.H. Kollins, E.K. MacDonald, C.R. Rush. Assessing the abuse potential of methylphenidate in nonhuman and human subjects - a review. *Pharmacol. Biochem. Behav.* **2001**, *68*, 611.
- [25] Q. Babcock, T. Byrne. Student perceptions of methylphenidate abuse at a public liberal arts college. *J. Am. Coll. Health* **2000**, *49*, 143.
- [26] J.F. Casale, P.A. Hays. Ethylphenidate: an analytical profile. *Microgram J.* **2011**, *8*, 58.
- [27] The Misuse of Drugs Act 1971 (Temporary Class Drug) Order 2015. S.I. No. 1027. Available [http://www.legislation.gov.uk/ukxi/2015/1027/pdfs/ukxi\\_20151027\\_en.pdf](http://www.legislation.gov.uk/ukxi/2015/1027/pdfs/ukxi_20151027_en.pdf) [09 September 2016].
- [28] Psychoactive Substances Act 2016. Chapter 2. Available [http://www.legislation.gov.uk/ukpga/2016/2/pdfs/ukpga\\_20160002\\_en.pdf](http://www.legislation.gov.uk/ukpga/2016/2/pdfs/ukpga_20160002_en.pdf) [09 September 2016].
- [29] H. Klare, J.M. Neudörfl, S.D. Brandt, E. Mischler, S. Meier-Giebing, K. Deluweit, F. Westphal, T. Laussmann. Analysis of six "neuro-enhancing" phenidate analogs. *Drug. Test. Anal.* **2017**, doi: 10.1002/dta.2161.
- [30] C. Parks, D. McKeown, H.J. Torrance. A review of ethylphenidate in deaths in east and west Scotland. *Forensic Sci. Int.* **2015**, *257*, 203.
- [31] J. Krueger, H. Sachs, F. Musshoff, T. Dame, J. Schaeper, M. Schwerer, M. Graw, G. Roider. First detection of ethylphenidate in human fatalities after ethylphenidate intake. *Forensic Sci. Int.* **2014**, *243*, 126.
- [32] P.D. Maskell, P.R. Smith, R. Cole, L. Hikin, S.R. Morley. Seven fatalities associated with ethylphenidate. *Forensic Sci. Int.* **2016**, *265*, 70.
- [33] J.S. Markowitz, C.L. Devane, D.W. Boulton, Z. Nahas, S.C. Risch, F. Diamond, K.S. Patrick. Ethylphenidate formation in human subjects after the administration of a single dose of methylphenidate and ethanol. *Drug Metab. Dispos.* **2000**, *28*, 620.
- [34] Irish Statute Book. Criminal Justice (Psychoactive Substances) Act 2010. Available at: <http://www.irishstatutebook.ie/eli/2010/act/22/enacted/en/pdf> [8 August 2016].
- [35] European Monitoring Centre for Drugs and Drug Addiction (EMCDDA). Early-Warning-System on New Drugs. 4-Fluoromethylphenidate. EMCDDA database on new drugs (EDND). **2015**. Restricted access.

- 1  
2  
3 [36] Bruker APEX2 v2014.11-0, Bruker AXS Inc., Madison, Wisconsin,  
4 USA, **2014**.
- 5 [37] G.M. Sheldrick. SHELXT - Integrated space-group and crystal-structure  
6 determination. *Acta Cryst.* **2015**, A71, 3.
- 7 [38] G.M. Sheldrick. A short history of SHELX. *Acta Cryst. A* **2008**, 64, 112.
- 8 [39] O.V. Dolomanov, L.J. Bourhis, R.J. Gildea, J.A.K. Howard, H.  
9 Puschmann. OLEX2: a complete structure solution, refinement and  
10 analysis program. *J. Appl. Crystallogr.* **2009**, 42, 339.
- 11 [40] G.M. Sheldrick. SADABS. Bruker AXS Inc., Madison, Wisconsin, USA,  
12 **2012**.
- 13 [41] R.B. Rothman, N. Vu, J.S. Partilla, B.L. Roth, S.J. Hufeisen, B.A.  
14 Compton-Toth, J. Birkes, R. Young, R.A. Glennon. In vitro  
15 characterization of ephedrine-related stereoisomers at biogenic amine  
16 transporters and the receptorome reveals selective actions as  
17 norepinephrine transporter substrates. *J. Pharmacol. Exp. Ther.* **2003**,  
18 307, 138.
- 19 [42] M.H. Baumann, M.A. Ayestas, J.S. Partilla, J.R. Sink, A.T. Shulgin,  
20 P.F. Daley, S.D. Brandt, R.B. Rothman, A.E. Ruoho, N.V. Cozzi. The  
21 designer methcathinone analogs, mephedrone and methylone, are  
22 substrates for monoamine transporters in brain tissue.  
23 *Neuropsychopharmacology.* **2012**, 37, 1192.
- 24 [43] Cayman Chemical. ( $\pm$ )-*threo*-Methylphenidate (hydrochloride) GC-MS.  
25 Available: [https://www.caymanchem.com/gcms/11639-0444273-](https://www.caymanchem.com/gcms/11639-0444273-GCMS.pdf)  
26 [GCMS.pdf](https://www.caymanchem.com/gcms/11639-0444273-GCMS.pdf) [09 November 2016].
- 27 [44] Cayman Chemical. ( $\pm$ )-*threo*-Ethylphenidate (hydrochloride) GC-MS.  
28 Available: [https://www.caymanchem.com/gcms/13896-0444213-](https://www.caymanchem.com/gcms/13896-0444213-GCMS.pdf)  
29 [GCMS.pdf](https://www.caymanchem.com/gcms/13896-0444213-GCMS.pdf) [09 November 2016].
- 30 [45] Cayman Chemical. ( $\pm$ )-*threo*-4-Fluoromethylphenidate (hydrochloride)  
31 GC-MS. Available: [https://www.caymanchem.com/gcms/9002651-](https://www.caymanchem.com/gcms/9002651-0480761-GCMS.pdf)  
32 [0480761-GCMS.pdf](https://www.caymanchem.com/gcms/9002651-0480761-GCMS.pdf) [09 November 2016]
- 33 [46] European Project Response. Analytical Report on 4FMPH. Available:  
34 [http://www.policija.si/apps/nfl\\_response\\_web/seznam.php](http://www.policija.si/apps/nfl_response_web/seznam.php) [9 November  
35 2016].
- 36 [47] B.L. Flamm, J. Gal. The thermal decomposition of methylphenidate in  
37 the gas chromatograph mass spectrometer. *Biomed.Mass Spectrom.*  
38 **1975**, 2, 281.
- 39 [48] K. Tsujikawa, Y.T. Iwata, M.Inoue, S. Higashibayashi, H. Inoue. Letter  
40 to the Editor: Comments "Characterization of four new designer drugs,  
41 5-chloro-NNEI, NNEI indazole analog, alpha-PHPP, alpha-POP, with  
42 11 newly distributed drugs in illegal products. *Forensic Sci. Int.* **2015**,  
43 251, 15.
- 44 [49] Froimowitz, M., Wu Kuo-Ming, George, C., VanDerveer, D., Shi Qing,  
45 Deutsch H.M. *Struct.Chem.* **1998**, 9, 295-303.
- 46 [50] M.M. Schweri, H.M. Deutsch, A.T. Massey, S.G. Holtzman.
- 47  
48  
49  
50  
51  
52  
53  
54  
55  
56  
57  
58  
59  
60

Biochemical and behavioural characterization of novel methylphenidate  
analogs. *J. Pharmacol. Exp. Ther.* **2002**, 301, 527.

For Peer Review

1  
2  
3  
4  
5  
6  
7  
8  
9  
10  
11  
12  
13  
14  
15  
16  
17  
18  
19  
20  
21  
22  
23  
24  
25  
26  
27  
28  
29  
30  
31  
32  
33  
34  
35  
36  
37  
38  
39  
40  
41  
42  
43  
44  
45  
46  
47  
48  
49  
50  
51  
52  
53  
54  
55  
56  
57  
58  
59  
60

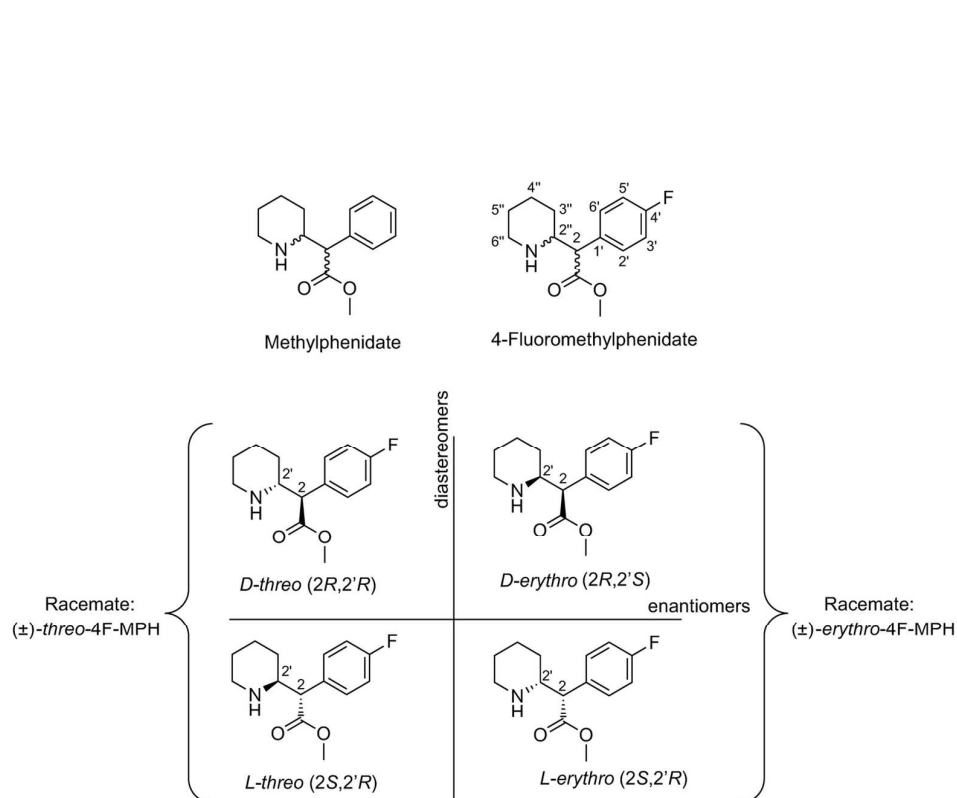


Figure 1. Chemical structures of methylphenidate, (±)-*threo*-racemate and (±)-*erythro*-racemate of 4-fluoromethylphenidate

134x88mm (300 x 300 DPI)

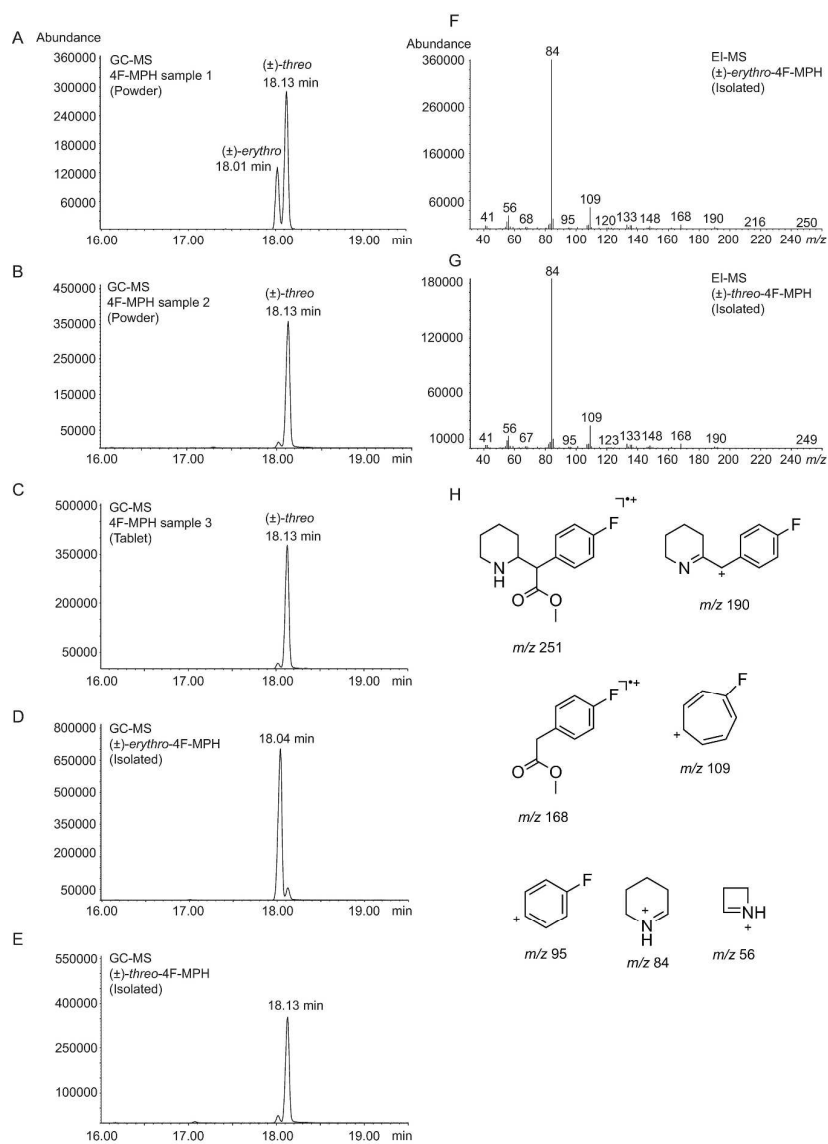


Figure 2. A-E: Gas chromatographic (GC) separation obtained for the isolated  $(\pm)$ -threo-racemate, isolated  $(\pm)$ -erythro-racemate of 4F-MPH and vendor samples. F-G: Electron ionization mass spectra obtained for the isolated  $(\pm)$ -threo- and  $(\pm)$ -erythro- racemates of 4F-MPH. H: Proposed fragmentation pattern for both racemates.

281x391mm (300 x 300 DPI)

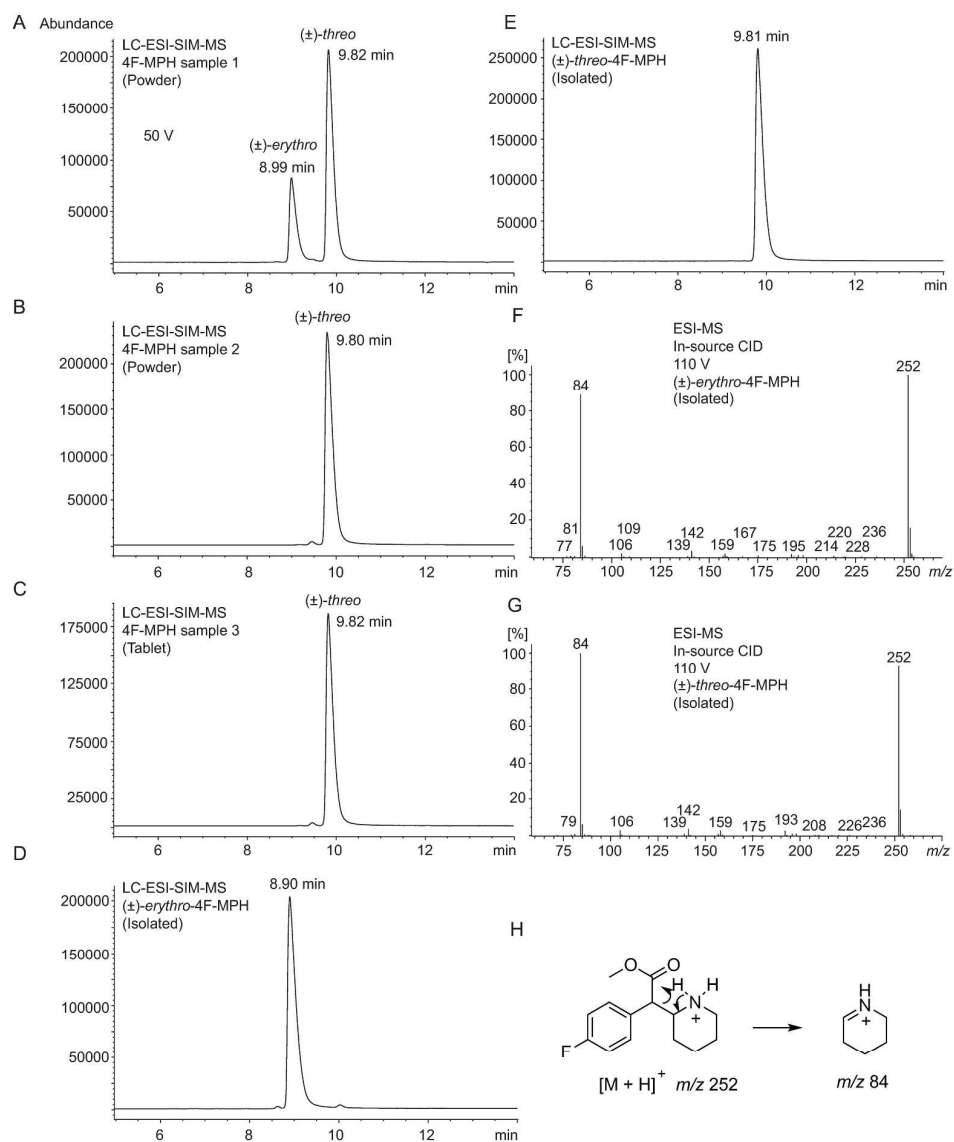
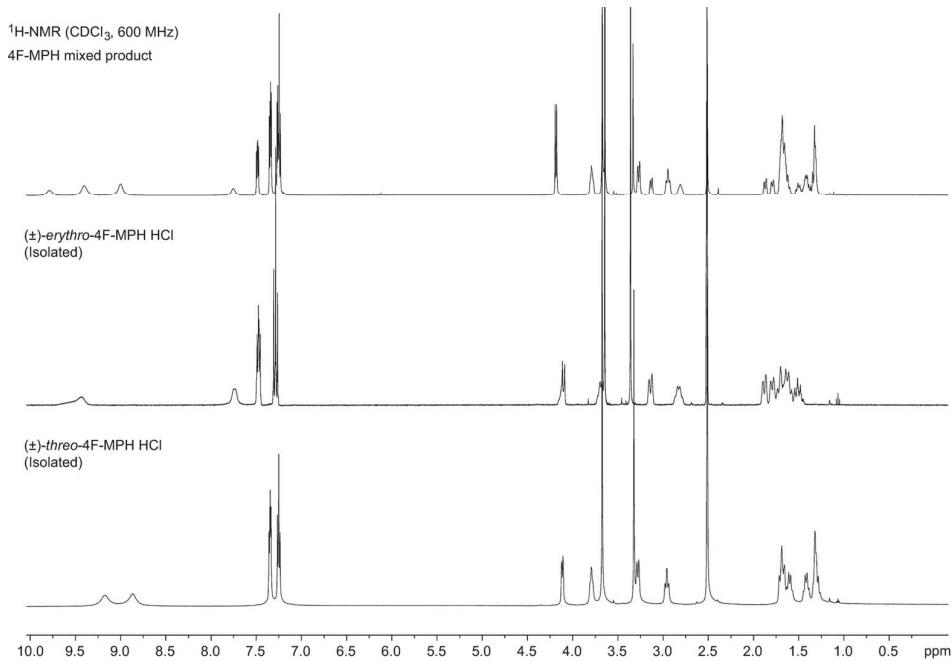


Figure 3. A-E: HPLC separation achieved for the isolated  $(\pm)$ -threo-racemate, isolated  $(\pm)$ -erythro-racemate and vendor samples of 4F-MPH. F-G: Product ion spectra obtained for isolated  $(\pm)$ -threo- and  $(\pm)$ -erythro-racemates of 4F-MPH obtained from in-source collision induced dissociation at increased fragmentor voltage (110 V). H: Proposed fragments for both racemates.

246x297mm (300 x 300 DPI)



30  
31  
32  
33  
34  
35  
36  
37  
38  
39  
40  
41  
42  
43  
44  
45  
46  
47  
48  
49  
50  
51  
52  
53  
54  
55  
56  
57  
58  
59  
60

Figure 4. <sup>1</sup>H NMR spectra obtained for the mixed 4F-MPH product, the isolated (±)-*threo*-racemate and isolated (±)-*erythro*-racemates of 4F-MPH.

142x98mm (300 x 300 DPI)

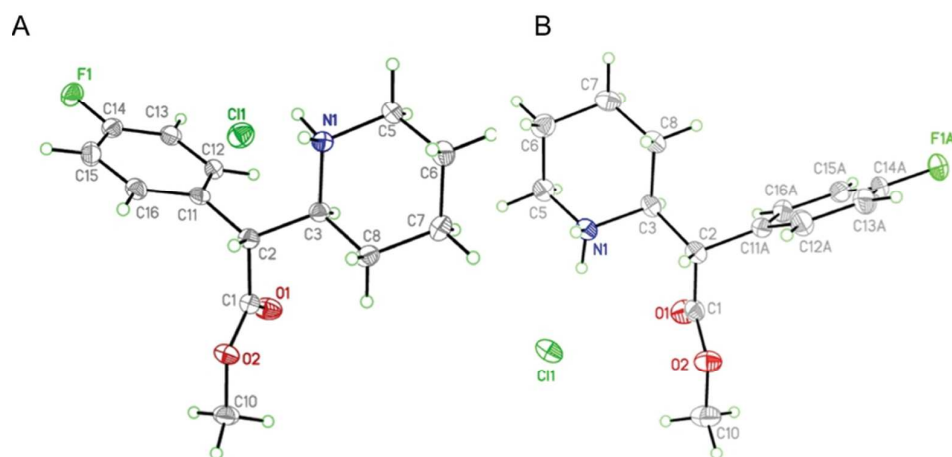


Figure 5. A: Structure of (±)-*erythro* and B: (±)-*threo* salts of 4F-MPH. Atomic displacement parameters shown at 50% probability and hydrogen atoms drawn as spheres of arbitrary radius. In B, only the major disordered fluorophenyl moiety is shown.

81x38mm (300 x 300 DPI)



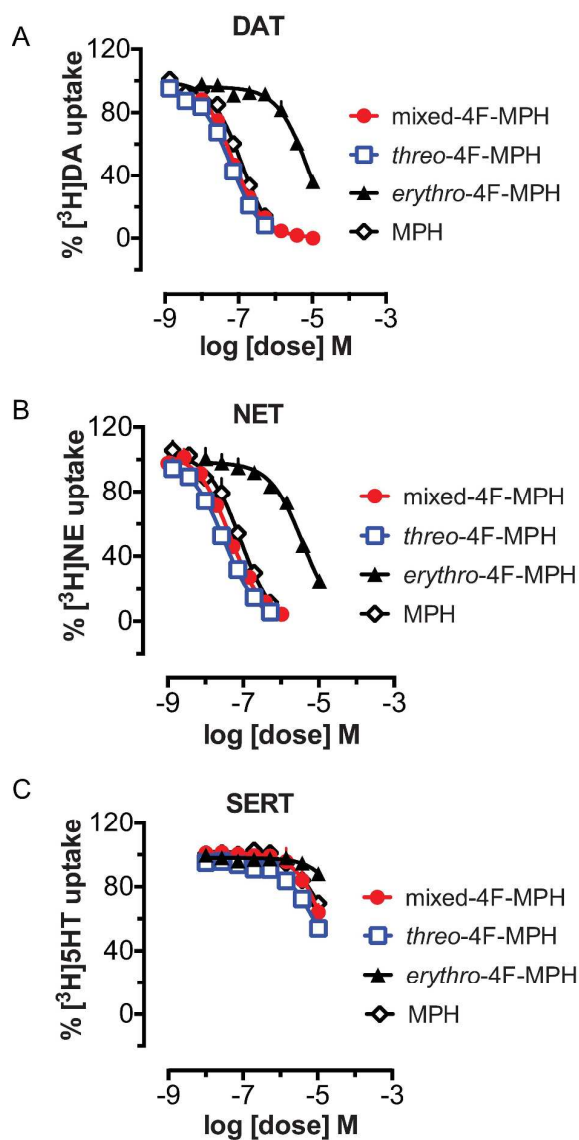


Figure 6. Effects of 4-fluoromethylphenidate isomers (4F-MPH) and comparison with methylphenidate (MPH) on inhibition of uptake at DAT, NET, and SERT in rat brain synaptosomes. Synaptosomes were incubated with different concentrations of test drugs in the presence of 5 nM [ $^3\text{H}$ ]dopamine (A, for DAT), 10 nM [ $^3\text{H}$ ]norepinephrine (B, for NET), or 5 nM [ $^3\text{H}$ ]serotonin (C, for SERT). Data are percentage of [ $^3\text{H}$ ]transmitter uptake expressed as mean  $\pm$  s.e.m. for  $n = 3$  experiments.

242x486mm (300 x 300 DPI)

1  
2  
3  
4  
5  
6  
7  
8  
9  
10  
11  
12  
13  
14  
15  
16  
17  
18  
19  
20  
21  
22  
23  
24  
25  
26  
27  
28  
29  
30  
31  
32  
33  
34  
35  
36  
37  
38  
39  
40  
41  
42  
43  
44  
45  
46  
47  
48  
49  
50  
51  
52  
53  
54  
55  
56  
57  
58  
59  
60

Test Drug	[ <sup>3</sup> H]DA uptake via DAT IC <sub>50</sub> (nM)	[ <sup>3</sup> H]NE uptake via NET IC <sub>50</sub> (nM)	[ <sup>3</sup> H]5-HT uptake via SERT IC <sub>50</sub> (nM)
Diastereomeric mixture of 4F-MPH	66.35 ± 3.27	44.6 ± 4.17	>10,000
(±)- <i>threo</i> -4F-MPH	60.96 ± 4.6	30.68 ± 2.64	8,805 ± 2475
(±)- <i>erythro</i> -4F-MPH	8,528 ± 1753	3,779 ± 570.5	>10,000
MPH	131.0 ± 14.2	82.85 ± 11.145	>10,000

<sup>a</sup> Data are expressed as nM concentrations (mean ± SD) for n = 3 separate experiments performed in triplicate. For dose-response curve, see Figure 6.